The calcilytic drug Calhex-231 ameliorates vascular hyporesponsiveness in traumatic hemorrhagic shock by inhibiting oxidative stress and mitochondrial fission

Yan Lei
Army Medical University
Xiaoyong Peng
Army Medical University
Tao Li
Army Medical University
Liangming Liu
Army Medical University
Guangming Yang (yanggm971@163.com)
Research Institute of Surgery

Research

Keywords: Calcium-sensing receptor, Calhex-231, traumatic hemorrhagic shock, vascular hyporesponsiveness, mitochondrial fusion-fission

Posted Date: February 18th, 2020

DOI: https://doi.org/10.21203/rs.2.23868/v1

Abstract

Background The calcium-sensing receptor (CaSR) plays a fundamental role in extracellular calcium homeostasis in humans. Surprisingly, CaSR is also expressed in non-homeostatic tissues and is involved in regulating diverse cellular functions. The objective of this study was to determine if Calhex-231 (Cal), a negative modulator of CaSR, may be beneficial in the treatment of traumatic hemorrhagic shock (THS) by improving cardiovascular function, and investigated its relationship to oxidative stress and the mitochondrial fusion-fission pathway.

Methods Rats that had been subjected to traumatic hemorrhagic shock were used as models in this study. Hypoxia-treated vascular smooth muscle cells (VSMCs) were also used. The effects of Cal on cardiovascular function, animal survival, hemodynamic parameters, and vital organ function in THS rats were observed, and the relationship to oxidative stress and mitochondrial fusion-fission was investigated.

Results Cal significantly improved hemodynamics, elevated blood pressure, increased vital organ blood perfusion and local oxygen supply, and markedly improved the survival outcomes of THS rats. Furthermore, Cal significantly improved vascular reactivity after THS, including the pressor response of THS rats to norepinephrine (NE), and also the contractile response of superior mesenteric arteries, mesenteric arterioles, and isolated VSMCs to NE. Cal also restored the THS-induced decrease in myosin light chain (MLC) phosphorylation, which is the principal mechanism responsible for VSMC contraction and vascular reactivity. Inhibition of MLC phosphorylation antagonized the Cal-induced restoration of vascular reactivity following THS. Cal decreased oxidative stress indexes and increased antioxidant enzyme levels in THS rats, and also reduced reactive oxygen species levels in hypoxic VSMCs. In addition, THS induced expression of mitochondrial fission proteins Drp1 and Fis1, and decreased expression of mitochondrial fusion protein Mfn1 in vascular tissues. Cal reduced expression of Drp1 and Fis1, but did not affect Mfn1 expression. In hypoxic VSMCs, Cal inhibited hypoxia-induced mitochondrial fragmentation and preserved mitochondrial morphology.

Conclusions Calhex-231 exhibits outstanding potential for effective therapy of traumatic hemorrhagic shock, due to its ability to improve hemodynamics, increase vital organ blood perfusion, and markedly prolong animal survival. These beneficial effects result from its protection of vascular function via inhibition of oxidative stress and mitochondrial fission.

Background

Trauma is the leading cause of death for people under 44 years of age, claiming more than 5 million victims per year worldwide [1]. About 40% of trauma-related mortality is attributed to hemorrhage and its sequelae [2]. Despite the development of new technologies and therapeutic methods in recent years, the management of trauma patients with severe hemorrhage and hemorrhagic shock remains a challenge. Cardiovascular dysfunction, such as vascular hyporesponsiveness, is a well-documented phenomenon and a major cause of death in trauma patients with severe hemorrhage or hemorrhagic shock. Vascular

hyporesponsiveness is characterized by an impaired response of blood vessels to vasoactive agents, which leads to refractory hypotension and multiple organ failure, even when the patient is supported by traditional fluid resuscitation and vasopressors [3–6]. In order to develop more effective treatments, it is necessary to investigate the underlying mechanisms of vascular hyporesponsiveness in trauma and hemorrhagic shock.

The calcium-sensing receptor (CaSR), a member of the C family of G protein-coupled receptors (GPCR), plays a fundamental role in extracellular calcium homeostasis in humans by regulating parathyroid hormone (PTH) secretion and renal calcium reabsorption [7, 8]. Surprisingly, CaSR is also expressed outside of the parathyroid gland and kidney in non-homeostatic neural and cardiovascular tissues. In the cardiovascular system, functional CaSR is present in cardiomyocytes, perivascular nerves, vascular endothelial cells (VECs), and vascular smooth muscle cells (VSMCs) [9]. Several studies have shown that CaSR plays an important role in the regulation of vascular tone and blood pressure [8–11]. However, the precise mechanism by which CaSR regulates blood pressure has not been determined.

CaSR can be activated by many kinds of ligands in addition to extracellular calcium (Ca_o^{2+}), the prototypical activator of CaSR. Type I agonists include cations such as $Mg^{2+}$and Gd^{3+}, polyamines, and some antibiotics. In addition to these biological ligands, a series of type II allosteric modulators of CaSR have been developed. Positive allosteric modulators of CaSR, such as Cinacalcet and Calindol, are named calcimimetics, while negative modulators of CaSR, such as NPS2143 and Calhex-231, are named calcilytics [12–14]. Cinacalcet is the only allosteric CaSR modulator that is currently approved for use in humans, and is used to treat uraemic secondary hypercalcaemia and secondary hyperparathyroidism caused by chronic kidney disease [13]. Calcilytics inhibit CaSR and stimulate PTH secretion, and are thus potential treatments for osteoporosis [14]. Recently, some studies on the effect of calcimimetics and calcilytics in the vasculature suggest that CaSR modulators may have therapeutic potential in the treatment of cardiovascular disease [15, 16]. However, it is unknown whether CaSR is involved in trauma/shock-induced cardiovascular dysfunction, or if CaSR modulators might exert protective effects on cardiovascular function during traumatic shock.

Oxidative stress and mitochondrial dysfunction play critical roles in the pathogenesis of many cardiovascular diseases, such as atherosclerosis, ischemic heart disease, and hypertension. An increased understanding of the tight link between oxidative stress and mitochondria offers tantalyzing prospects for the treatment and prevention of these diseases [17]. Oxidative stress is an imbalance in the production of oxidants and antioxidants. Reactive oxygen species (ROS) are produced during oxidative stress and are involved in multiple organ damage in patients experiencing severe trauma and hemorrhage. While mitochondria are the primary source of ROS, ROS also cause mitochondrial damage and dysfunction. Mitochondrial function is closely linked to the balance between the opposing processes of mitochondrial fusion and fission. In mammalian cells, the primary regulators of mitochondrial fission are dynamin-related protein 1 (Drp1) and fission 1 (Fis1), whereas mitochondrial fusion is regulated by mitofusin 1 (Mfn1) and mitofusin 2 (Mfn 2). Interactions between ROS and mitochondrial dynamic fusion-fission have been implicated in aging, cancer, neuropathies, and cardiovascular disorders [18, 19].

We previously showed that oxidative stress and mitochondrial dysfunction are both involved in the pathogenesis of vascular hyporesponsiveness following shock. The damage caused by ROS may be due to an impairment of mitochondrial permeability [6], which is closely related to the status of mitochondrial fusion-fission. Based on the literature and our previous findings, we hypothesized that CaSR and its modulators play important roles in cardiovascular function, possibly via a mechanism that is related to oxidative stress and mitochondrial dynamic processes.

In this study, we tested whether the calcilytic (negative modulator of CaSR) Calhex-231 improves cardiovascular function when used to treat traumatic hemorrhagic shock (THS). We also investigated the relationship between oxidative stress and the mitochondrial fusion-fission pathway, using traumatic hemorrhagic shock-induced rats and hypoxia-treated vascular smooth muscle cells (VSMCs).

Methods

Animals

This study was approved by the Laboratory Animal Welfare and Ethics Committee Of the Third Military Medical University. All experiments conformed to the “Guide for the Care and Use of Laboratory Animals” (Eighth Edition, 2011, Washington, D.C., National Academies Press, USA). Three hundred and eighty male and female Sprague–Dawley (SD) rats (190–220 g) were housed in a containment facility at the animal center at an ambient temperature of 25 °C and a light/dark cycle of 12 hr each. Animals were provided with food and water *ad libitum*. Food was withdrawn 12 hr prior to the experiment, but access to water was maintained.

Traumatic hemorrhagic shock models and resuscitation

Rats were anesthetized with sodium pentobarbital (initial dosage, 30 mg/kg ip) and Jingsongling (xylidinothiazole; initial dosage, 0.1 mg/kg im). The heparinized catheters were placed in the right femoral artery and vein. Blood pressure and bleeding were monitored from the femoral artery and drugs were administered through the femoral vein. The right carotid artery and vein were catheterized for monitoring hemodynamic values or cardiac output. Traumatic hemorrhagic shock was induced as previously described [6]. Briefly, a fracture of the left femur was made, and hemorrhage was induced via the right femoral artery catheter until mean arterial pressure (MAP) decreased to 30 mmHg. After maintaining this pressure for 2 hours, traumatic hemorrhagic shock was established and experiments were conducted. At the conclusion of all experiments, animals were euthanatized with a pentobarbital-based euthanasia solution (Sleepaway, 2 ml iv; Fort Dodge Laboratories, Fort Dodge, IA, USA).

For *in vivo* experiments, rats were randomly divided into six groups: normal control (sham- operated), shock control, shock+lactated Ringer’s (LR) solution, and shock+LR+Calhex-231 at 0.1, 1, or 5 mg/kg (Tocris Bioscience, Bristol, UK). When shock had been established, the animals in the three Calhex-231 (Cal) groups received a continuous infusion of 0.1, 1, or 5 mg/kg Cal in LR solution within 30 minutes. The LR group received only lactated Ringer’s solution. In these groups the volume of LR was twice the

volume of blood lost. The shock control group did not receive any treatment after shock. The sham-operated rats experienced the same operation but no shock was induced and they received no LR infusion. LR was administered with an infusion pump (Model AS 50, B. Braun Melsungen AG, Germany).

Animal survival

Ninety-six rats were randomly divided into the six groups (n=16/group) and subjected to the procedures described above. After resuscitation and group-specific treatments, all catheters were removed and the incisions were closed in two layers with nonabsorbable suture. Rats were returned to their cages and allowed free access to food and water. Postoperative analgesia (xylidinothiazole 0.2 mg/kg) was administered intramuscularly every 6 hr. Rats were observed every 1 hr for 24 hours.

Blood pressure and hemodynamics

Forty-eight rats were randomly divided into the six groups (n=8/group) and subjected to the procedures described earlier. Mean arterial pressure (MAP), the pressor response of norepinephrine (NE), and hemodynamic parameters were measured before hemorrhage (baseline), at the end of the shock period, and at 1 and 2 hours after resuscitation. MAP was monitored using the right femoral artery catheter connected to a blood pressure analyzer. The pressor response was represented as the maximum increase in MAP after administration of NE (3 μg/kg bolus intravenous injection), which reflects the *in vivo* systemic vascular reactivity. Hemodynamic parameters, including LVSP (left intraventricular systolic pressure), and $\pm dp/dt_{max}$ (maximal rate of change in left intraventricular pressure) were determined with a polygraph physiologic recorder (SP844; AD Instruments, Castle Hill, Australia).

Cardiac output and myocardial contractility

Forty-eight rats were used for this experiment, randomly divided into six groups and subjected to the procedures described above. Using a Cardiomax-III Thermodilution Cardiac Output System (Columbus Instruments, Columbus, OH, USA), cardiac output (CO) was measured at baseline, at the end of the shock period, and at 1 and 2 hr after resuscitation. Subsequently, rats were euthanatized and the hearts were immediately isolated and placed in Tyrode's solution (mmol/L: 137 NaCl, 5.4 KCl, 1.2 $MgCl_2$, 10 HEPEs, 1.2 $CaCl_2$, 1.2 NaH_2PO_4, 10 glucose), continuously infused with 95 % O_2 / 5 % CO_2. A papillary muscle bundle was dissected from the left ventricle and mounted in an organ bath continuously perfused with oxygenated Tyrode's solution for 2 hr at 30 ºC. Papillary muscles were electrically stimulated by 10 ms square wave pulses at a rate of 0.2 Hz and a voltage 20 % above threshold. After equilibration for 1 hr at a resting tension of 0.5 g, the muscles were adjusted to optimum length, followed by another 30 min period of equilibration. Contractility of the isolated papillary muscle was analyzed under increasing isoproterenol concentrations (10^{-9} to 10^{-4} mol/L), and the contractile force was recorded with a Power Lab System via a force transducer (AD Instruments, Castle Hill, Australia). Papillary muscle contractility, normalized for muscle cross-sectional area (g/mm^2), was calculated using the formula: $G/\pi(D/2)^2$ (G: tension; D: diameter).

Vital organ blood perfusion, local oxygen supply, and vascular reactivity of isolated mesenteric vessels

Forty-eight rats were divided into six groups (n=8/group) and subjected to the treatments described above. Two hours after resuscitation, blood perfusion of the liver and kidney was assessed by laser speckle contrast analysis (LASCA) using a PeriCam PSI system (PSI-ZR; Perimed, Jarfalla, Sweden). Briefly, the rats were placed in the supine position, sodium pentobarbital and xylidinothiazole anesthesia was maintained, and a laparotomy was performed exposing the liver and kidney. Dynamic blood perfusion was recorded in real-time with a PSI camera, and the data were expressed as perfusion units (PU) calculated using PIMSoft version 1.5 (Perimed). Subsequently, oxygen saturation of the liver and kidney was assessed by tissue spectrophotometry using an “oxygen to see” (O2C) system (LEA Medizintechnik, Giessen, Germany). The O2C probe was placed on the surface of the liver and kidney, and the capillary venous oxygen saturation was recorded.

After these procedures, rats were euthanized and the superior mesenteric arteries (SMAs) were rapidly excised and placed in ice-cold Krebs-Henseleit (K-H) solution. SMAs were sectioned into rings 2-3 mm long, and the endothelium was denuded by gently rubbing the intimal surface as previously described [3]. The vascular contraction function to NE was measured using an isolated organ perfusion system (Scientific Instruments, Barcelona, Spain). Maximal contraction (Emax) and NE concentration-response curves were used to compare vascular reactivity.

A cohort of twenty-four rats was divided into three groups (n=8/group): shock+LR+Cal 1 mg/kg, shock+LR+Cal+ML-9 10^{-6} mol/L (a selective MLCK inhibitor, Sigma, St. Louis, MO, USA), and shock+LR+Cal+ML-9 5×10^{-6} mol/L. The procedures, including production of the shock model, Cal treatment, and isolation of SMA rings were identical to those described above. Some SMA rings were treated with ML-9 10^{-6} mol/L or 5×10^{-6} mol/L for 30 min before reactivity to NE was determined.

Microvascular reactivity of mesenteric microvessels *in vivo*

Thirty-two rats were randomly divided into four groups (n=8/group): normal control, shock control, shock+LR, and shock+LR+Cal 1 mg/kg. Two hours after resuscitation, the rats were placed in the lateral position. A 2~3-cm-long midline abdominal incision was made, and the small intestine near the cecum was exteriorized gently and placed on a transparent observation board. The mesenteric microvessels were observed under an inverted intravital microscope (BX51WI, Olympus, Tokyo, Japan) within a thermocontrolled box (37°C). Single unbranched arterioles with diameter between 30 to 50 μm and length ~200 μm were selected for study. The contractile response of mesenteric arterioles was assessed by measuring the change in diameter in response to increasing doses of NE (10^{-9}, 10^{-8}, 10^{-7}, and 10^{-6} mol/L). The videos and images of arterioles were recorded using a microscope equipped with a CCD camera (DP21, Olympus). Arteriole diameters were measured with the Image-Pro Plus 5.0 application (Media Cybernetics, Silver Spring, MD). Changes in diameter were calculated using the expression $(D_1-D_2)/D_1\times100\%$ (D_1 and D_2: diameter before and after the addition of NE, respectively).

Isolation of cardiomyocytes and VSMCs, and contraction in isolated myocytes

Thirty-two rats were randomly divided into four groups (n=8/group): normal control, shock control, shock+LR, and shock+LR+Cal 1 mg/kg. Two hours after resuscitation, hearts and mesenteric arteries were rapidly removed. Dissociated cardiomyocytes were isolated by a collagenase perfusion method. Briefly, the hearts were mounted in a Langendorff perfusion apparatus, and perfused with Ca^{2+}-free perfusion buffer (mmol/L: NaCl 137, KCl 5.4, $MgCl_2$ 1.2, HEPES 10, glucose 10, pH 7.4) containing 10 mmol/L taurine for 7 min, then switched to oxygenated digestion buffer (perfusion buffer containing 2 g/L collagenase type II, 2 g/L bovine serum albumin, and 25 μmol/L $CaCl_2$) for 19 min. Hearts were then perfused with perfusion buffer to terminate the digestion. After perfusion, the ventricles were pulled into small pieces in Krebs buffer (KB) solution, and the tissues were gently dispersed to generate a cell suspension using a plastic pipette. Cardiomyocytes were harvested by filtration through a 100-mesh cell strainer, centrifuged at 500 rpm for 40 s, and then washed sequentially with buffers containing, 0.4, 0.8, and 1.2 mmol/L $CaCl_2$. Cardiomyocytes contraction was observed using an IonOptix edge-detection system (IonOptix LLC, Milton, MA, USA) [20].

Dissociated smooth muscle cells were freshly isolated using an enzymatic method. Briefly, after dissection and removal of endothelium, the mesenteric arteries were cut into 2 mm segments, and then incubated for 30 min at 37°C with gentle shaking in a Ca^{2+}-free physiological salt solution (PSS, mmol/L: NaCl 127, KCl 5.9, $MgCl_2$ 1.2, HEPES 10, glucose 12, pH 7.4) containing 2 g/L collagenase type II, 4 g/L papain, 2 g/L bovine serum albumin, and 1 mmol/L dithiothreitol. The partly digested tissues were rinsed three times with Ca^{2+}-free PSS and gently agitated with a plastic pipette in low-Ca^{2+} (20 μmol/L) PSS. The dissociated cells were harvested by filtration through a 100-mesh cell strainer, and then stored at 4°C until used (within 4-h following dispersion). The contractile response to NE (measured as change in length) of isolated VSMCs was determined using a Leica TCS SP5 confocal system (Leica Microsystems, Wetzlar, Germany).

Oxidative stress assay, preparation of tissue lysates, and western blot analysis

Thirty-two rats were divided into four groups (n=8/group), and treated as described above. Two hours after resuscitation, blood samples and SMA tissues were collected. Serum levels for four oxidative stress biomarkers, including malondialdehyde (MDA), superoxide dismutase (SOD), catalase (CAT), and glutathione (GSH), were detected with commercial assay kits (Jiancheng Bioengineering Institute, Nanjing, China) according to the manufacturer's instructions. SMA tissue protein extracts were prepared and western blot analysis was performed as described previously [3]. Antibodies were as follows: MLC (myosin light chain, 1:1000; Sigma), phospho-MLC (1:1000; Cell Signaling, Danvers, MA, USA), Drp1 (1:1000; Abcam, Cambridge, MA, USA), Fis1 (1:1000; Abcam), Mfn1 (1:1000; Abcam), Mfn2 (1:1000; Abcam), and β-actin (1:5000; Sigma). Bands were detected with fluorescent secondary antibodies and quantified using the Odyssey CLx Infrared Imaging System (LI-COR, Inc., Lincoln, Nebraska, USA).

Primary culture of VSMCs and hypoxic treatment

Rat VSMCs were obtained from the SMAs of twenty adult SD rats using an explant technique as previously described [3]. VSMCs were cultured in Dulbecco's modified Eagle medium-F12 supplemented with 20% fetal bovine serum (Hyclone, Logan, UT, USA) and 1% antibiotics. Cells from passages 3 to 5 were used in the study. For hypoxic challenge, VSMCs were transferred into a hypoxia culture compartment (MIC-101, Billups-Rothenberg Inc., Del Mar, CA, USA), equilibrated by bubbling with 95% N_2 and 5% CO_2 for 15 min and then allowed to sit for 10 min. This procedure was repeated five times until the oxygen concentration was < 0.2%. VSMCs were maintained under hypoxic conditions for 2 hr and then used for subsequent experiments.

ROS level in VSMCs

Reactive oxygen species (ROS) levels in VSMCs were measured using the 2',7'-dichlorofluorescin diacetate (DCF-DA) method [6]. The cultured VSMCs were divided into three groups: normal control, hypoxia 2-h, and hypoxia+Cal (10 μmol/L, 30 min). After treatment with hypoxia and/or Cal, VSMCs were incubated with 10 μmol/L DCF-DA (Sigma) for 20 min at 37°C. DCF fluorescence was detected at 488 nm excitation and 525 nm emission using a Leica TCS SP5 confocal microscope. Images were collected and the mean fluorescence intensities of DCF were measured using the Image J application.

Mitochondrial morphology

To visualize mitochondria in living cells, a mitochondria-specific probe was used. The VSMCs were divided into 3 groups: normal control, hypoxia 2-h, and hypoxia+Cal. After being subjected to hypoxia and/or treated with Cal, the VMSCs were washed with PBS and loaded with 100 nmol/L of MitoTracker deep red (Sigma) for 30 minutes. Fluorescence was detected with an excitation of 633 nm using a Leica confocal microscope.

Statistical analysis

Data are presented as means ± standard error (SEM). Animal survival was analyzed using the Kaplan-Meier survival curve, and the differences among groups were analyzed using a chi-square test. For the other experiments, differences between experimental groups were assessed using one or two-factor analysis of variance analyses, followed by *post-hoc* Tukey tests. Statistical calculations were performed using SPSS 18.0 (SPSS Inc., Chicago, IL). $P<0.05$ was the threshold for statistical significance.

Results

1. **Effect of Calhex-231 on survival time and 24-hr survival rate in rats with THS**

Administration of 5 or 1 mg/kg Cal significantly increased survival time and the 24-hr survival rate of rats suffering traumatic hemorrhagic shock (P<0.01). The survival time and 24-hr survival rate in these two groups were statistically indistinguishable. Rats in the 0.1 mg/kg Cal group had slightly increased survival time and 24-hr survival rate compared to rats in the LR only group, but the difference was not statistically significant (Fig. 1A, B).

Fig. 1

2. **Effect of Calhex-231 on blood pressure and hemodynamics in rats with THS**

In all groups, mean arterial pressure, LVSP, and $\pm dp/dt_{max}$ decreased significantly after shock. Administration of 5 or 1 mg/kg Cal resulted in significantly increased MAP 2 hr post administration and hemodynamic values at 1 and 2 hr post administration, compared to rats in the LR only group (P<0.05 or 0.01). Rats treated with 1 mg/kg Cal demonstrated the greatest recovery; at 2-hr post administration, MAP, LVSP, and $\pm dp/dt_{max}$ in this group were restored to 65.0%, 85.9%, 90.6%, and 80.4%, respectively, of normal control levels. In the shock control rats, MAP and hemodynamic values remained depressed or decreased slightly 1 and 2 hr after shock (Fig. 2A–D).

Fig. 2

3. **Effect of Calhex-231 on blood perfusion and oxygen saturation of liver and kidney in rats with THS**

A significant decrease in blood perfusion in liver and kidney was observed after shock. Administration of 5 or 1 mg/kg Cal resulted in significantly increased perfusion in both liver and kidney, compared to rats in the LR group (P<0.01). There was no statistical difference between the 5 and 1 mg/kg Cal groups, nor was there between the 0.1 mg/kg and LR groups (Fig. 3A-C). Not unexpectedly, the oxygen saturation results mirrored the blood perfusion results (Fig. 3D, E).

Fig. 3

4. **Effect of Calhex-231 on cardiac function in rats with THS**

Cardiac function was evaluated *in vivo* by measuring cardiac output and *in vitro* by measuring the contractility of isolated ventricular papillary muscle and single cardiomyocytes. Cardiac output decreased significantly after shock. In all treatment groups, CO returned to near baseline levels 1 hr after treatment commenced and remained steady thereafter. Two hr after the beginning of treatment, CO in the LR group was about 92.9% of normal control levels. Cal did not further increase the CO, and there was no statistical difference between the Cal and the LR groups (Fig. 4A). Similar results were observed *in vitro*. Contractility of isolated papillary muscle and single cardiomyocytes from THS rats also decreased significantly, while contractility significantly increased in the LR group. No significant differences were observed between the Cal and the LR groups (Fig. 4B-D).

Fig. 4

5. **Effects of Calhex-231 on vascular function in rats with THS**

To determine the effects of Cal on vascular function (vascular reactivity) following THS, we investigated pressor effect of NE, and the contractile response of superior mesenteric arteries (SMA), mesenteric arterioles, and isolated VSMCs to NE *in vivo and in vitro*. The pressor effect of NE (reflecting vascular reactivity *in vivo*) in THS rats decreased significantly, consistent with our previous report [6]. LR infusion slightly improved the pressor response to NE. Cal treatments at 1 and 5 mg/kg significantly increased the pressor effect of NE as compared with the LR group (P<0.01) (Fig. 5A). Similarly, the constriction reactivity of isolated SMAs from THS rats was significantly reduced, and LR improved slightly. Treatment with Cal at 1 and 5 mg/kg markedly increased the constriction of SMAs from THS rats (Fig. 5B). Similar results were obtained in the mesenteric arterioles and isolated VSMCs. Cal at 1 mg/kg also significantly restored the decreased constriction reactivity of mesenteric arterioles and VSMCs to NE (Fig. 5C-F).

Fig. 5

6. **Effects of Calhex-231 on oxidative stress**

MDA, a product of lipid peroxidation, is a sensitive indicator of oxidative stress. MDA levels in blood samples from THS rats increased significantly. In parallel, levels of the protective antioxidant enzymes SOD, CAT, and GSH also increased. Levels of these biomarkers did not change significantly after resuscitation with LR alone. Administration of Cal at 1 mg/kg significantly decreased MDA level, and further increased CAT and GSH levels, as compared with the LR group (P<0.05 or 0.01). In contrast, Cal had no significant influence on SOD (Fig. 6A-D). Under hypoxic conditions, intracellular ROS levels in VSMCs increased significantly. Treatment with Cal markedly reduced ROS levels in hypoxic VSMCs (Fig. 6E and F).

Fig. 6

7. **Role of MLC phosphorylation in Cal-mediated effects on vascular reactivity after THS**

To determine whether MLC phosphorylation is involved in the regulation of Cal on vascular reactivity after shock, we investigated MLC protein expression and phosphorylation in SMA tissues from THS rats after Cal treatment. Immunoblot analysis revealed that the phosphorylation of MLC in blood vessels decreased significantly after shock, and LR infusion had no significant influence on MLC phosphorylation. Cal treatment significantly increased MLC phosphorylation, while MLC protein expression did not change (Fig. 7A-C). We also measured the effects of ML9 (a selective MLCK inhibitor that inhibits phosphorylation of MLC) on the Cal-induced increase in vascular reactivity in THS rats. Two doses of ML9 antagonized the Cal-induced restoration of vascular reactivity of SMA after shock (P<0.01). Relative to the group receiving Cal alone, the maximal contractile responses of SMA to NE in groups treated with Cal+ML9 10^{-6} mol/L and Cal+ML9 5×10^{-6} mol/L were 68.9% and 57.4%, respectively (Fig. 7D).

Fig. 7

8. **Effects of Calhex-231 on mitochondrial fission/fusion and mitochondrial morphology following THS**

Immunoblot analysis showed that expression of Drp1 and Fis1, two important mitochondrial fission proteins, increased significantly in blood vessels from THS rats. LR infusion further increased Drp1 and Fis1 levels. Cal treatment significantly reduced Drp1 and Fis1 expression (Fig. 8A-C). Expression of the fusion protein Mfn1 decreased significantly after shock, while LR infusion and Cal had no significant influence on Mfn1 levels under shock conditions (Fig. 8A, D). Expression of Mfn2, another fusion protein, did not change significantly after shock and/or Cal treatment (Fig. 8A, E).

To examine the effects of Cal treatment *in vitro*, VSMC mitochondria were stained with MitoTracker deep red. Confocal microscopy showed that hypoxia caused significant changes in mitochondrial morphology in rat VSMCs. Most mitochondria in normal cells were tubular, branched, and displayed a typical networked morphology. However, exposure to hypoxia disrupted the elongated networked structure, and mitochondria became shorter and fragmented. Treatment with Cal significantly reduced the hypoxia-induced mitochondrial fragmentation in VSMCs, as measured by the incidence of fragmented mitochondria and the formation of elongated networks (Fig. 8F).

Fig. 8

Discussion

Our results demonstrate that Calhex-231 (Cal), a specific inhibitor of CaSR, has a mitigating effect on traumatic hemorrhagic shock by improving vascular hyporesponsiveness and reducing mitochondrial dysfunction. First, application of Cal significantly improved survival outcomes in THS rats, stabilized hemodynamic values, and increased vital organ blood perfusion. Second, Cal exerts its protective effect by regulating vascular contraction and concomitant MLC phosphorylation in smooth muscle, thereby recovering vascular hyporesponsiveness after THS. Finally, the vascular function protection conferred by Cal may be attributed to attenuation of oxidative stress and reversal of damage to mitochondrial morphology and function. These findings show the important role played by CaSR in the regulation of vascular reactivity in THS, and the potential offered by its allosteric modulator Calhex-231 for the treatment of critical illness.

CaSR is known to control systemic calcium homeostasis in humans, and several synthetic CaSR modulators have been developed for the medical management of disorders of calcium metabolism [21]. Recently, CaSR expression has been conclusively demonstrated in various components of the cardiovascular system, including cardiomyocytes, vascular cells, and perivascular nerves, and has been shown to have a physiological role in the modulation of blood pressure [8–11]. The functions of CaSR and its modulators in cardiovascular physiology and pathophysiology have received much attention.

Several studies show that the calcimimetic drug R-568 induces a sustained reduction in blood pressure in uremic and spontaneously hypertensive rats but not in normal rats [22, 23]. The calcilytic compound NPS 2143 increases blood pressure in normotensive rats [24]. However, Fryer et al. [25] reported that Cinacalcet (also termed AMG073, the only calcimimetic approved for clinical use) produces an acute increase in blood pressure in both uremic and normal rats. In in vitro experiments, NPS 2143 inhibits vascular contraction induced by vasoconstrictors in rat mesenteric arteries exposed to hypoxia/reoxygenation [26]. These conflicting results may be related to the fact that CaSR is expressed in a diverse range of tissues, or that the experiments were conducted in different pathophysiologic states or used different methods for drug administration.

In this study, we first evaluated the therapeutic effects of intravenous infusion of the calcilytic drug Calhex-231 in rats subjected to traumatic hemorrhagic shock. After shock, the animals in the Cal groups received a continuous infusion of Cal with LR solution, delivered through the femoral vein by an infusion pump. Our results show that compared with resuscitation by LR alone, two doses of Cal (1 and 5 mg/kg) provide therapeutic benefit in traumatic hemorrhagic shock. The drug improved hemodynamic values, increased blood pressure, vital organ blood perfusion, and local oxygen supply, and markedly improved survival. Next, to investigate whether the cardiovascular actions of Cal contribute to its protective effects against hemorrhagic shock, we observed the effects of Cal on cardiac function and vascular function in vivo and in vitro. Our data showed that the indicators for heart function, including cardiac output in THS rats, and the contractility of isolated ventricular papillary muscle and single cardiomyocytes, decreased after shock. LR infusion significantly increased these indicators; while there were no significant differences in the Cal group compared with the LR group. Vascular function, the pressor response to NE, and the contractile response by superior mesenteric arteries, mesenteric arterioles, and isolated VSMCs to NE, are all decreased after shock. While LR infusion provides only slight improvement, Cal significantly increases these indicators. To investigate the relationship between CaSR and vascular reactivity, we measured the effects of Cal on MLC phosphorylation, since this is the principal mechanism responsible for VSMC contraction and vascular reactivity. We found that Cal treatment restores the shock-induced decrease in MLC phosphorylation in blood vessels. Moreover, ML9, a selective MLCK inhibitor that inhibits MLC phosphorylation, antagonized Cal-induced increase of vascular reactivity of SMA following THS. These results demonstrate that the calcilytic drug Calhex-231 has a beneficial effect on traumatic hemorrhagic shock by enhancing VSMC contraction and protecting vascular function.

To explore the mechanisms by which Calhex-231 improves vascular hyporesponsiveness following THS, we studied the relationships between the vascular action of Cal, oxidative stress, and mitochondrial dysfunction. Oxidative stress and mitochondrial dysfunction are correlated with pathogenesis in numerous cardiovascular diseases [17]. Oxidative stress results from an imbalance caused by excess production of oxidants (ROS) and damage to the ROS scavenging capacity provided by antioxidants (such as SOD and GSH). Mitochondria are not only the most important source of ROS, but they are also damaged by ROS excess [18, 19]. Our previous studies showed that oxidative stress plays an important role in the development of vascular hyporesponsiveness following hemorrhagic shock. We found that antioxidant therapy can regulate mitochondrial membrane permeability of VSMCs and improve

mitochondrial function after shock [6]. In the present study, levels of oxidative stress biomarkers, including MDA, SOD, CAT, and GSH, changed significantly after THS. Intracellular ROS levels in VSMCs also increased after hypoxia, confirming our previous observations [6]. Treatment with Cal decreased MDA levels and increased levels of antioxidant enzymes (CAT and GSH). Cal also markedly reduced ROS levels in hypoxic VSMCs, suggesting the calcilytic compound Calhex-231 has antioxidant activity.

We also found that hypoxia damages mitochondrial morphology and results in significant mitochondrial fragmentation in VSMCs. However, Cal treatment inhibits this fragmentation and preserves mitochondrial morphology. Mitochondria are highly dynamic, and their morphological changes correlate highly with function and cell fate. Mitochondrial morphology is regulated by the processes of fusion and fission. Some morphological regulatory factors have been identified in mammals, including the GTPases Drp1 and Fis1, which mediate mitochondrial fission, and the homologous GTPases Mfn1 and Mfn2, which mediate mitochondrial fusion [27, 28]. We therefore explored potential interactions between the vascular effects of Cal and mitochondrial fusion/fission proteins. Our data show that hemorrhagic shock increases the expression of mitochondrial fission proteins Drp1 and Fis1, and decreases the expression of the fusion protein Mfn1 in vascular tissues. Cal treatment reduces Drp1 and Fis1 expression, but does not affect Mfn1 expression. The results suggest that the protection conferred by Cal on mitochondrial morphology is due to inhibitory effects on the mitochondrial fission proteins Drp1and Fis1. In light of our previous studies and results reported by others, we speculate that Cal primarily protects vascular function by counteracting oxidative stress and mitochondrial fission. The precise mechanism by which Cal confers these benefits needs further investigation.

This study raises several important questions. Since CaSR is widely expressed in many tissues and organs, does it have additional anti-shock functions beyond those that result in vascular protection? Are these involved in the anti-shock effects of Calhex-231? What mechanisms are responsible for the crosstalk that occurs between oxidative stress and mitochondrial dysfunction? Can these mechanisms be exploited to develop novel treatment strategies for traumatic hemorrhagic shock?

Conclusions

In summary, our study demonstrates that the calcilytic drug Calhex-231 exhibits great potential as an effective therapeutic agent in the treatment of traumatic hemorrhagic shock. Cal treatment improves hemodynamic parameters and vital organ blood perfusion, and markedly prolongs survival in THS rats. The beneficial effects of Cal result from its ability to protect vascular function via inhibition of oxidative stress and mitochondrial fission.

Abbreviations

Cal: Calhex-231; CaSR: calcium-sensing receptor; CAT: catalase; Ca_o^{2+}: extracellular calcium; CO: cardiac output; DCF-DA:) 2',7'-dichlorofluorescin diacetate; ±dp/dtmax: maximal rate of change in left intraventricular pressure; Drp1: dynamin-related protein 1; Emax: Maximal contraction; Fis1: fission 1;

GPCR: G protein-coupled receptors; GSH: glutathione; HBP: hepatic blood perfusion; KB: Krebs buffer; K-H solution: Krebs-Henseleit solution; LASCA: laser speckle contrast analysis; LR solution: lactated Ringer's solution; LVSP: left intraventricular systolic pressure; MA: mesenteric arterioles; MAP: mean arterial pressure; MDA: malondialdehyde; Mfn1: mitofusin 1; Mfn 2: mitofusin 2; NE: norepinephrine; PM: papillary muscle; PSS: physiological salt solution; PTH: parathyroid hormone; PU: perfusion units; RBP: renal blood perfusion; ROS: Reactive oxygen species; SD rats: Sprague–Dawley rats; SEM: standard error; SMAs: superior mesenteric arteries; SOD: superoxide dismutase; THS: traumatic hemorrhagic shock; VECs: vascular endothelial cells; VSMCs: vascular smooth muscle cells.

Declarations

Ethics approval

This study was approved by the Laboratory Animal Welfare and Ethics Committee Of the Third Military Medical University. All experiments conformed to the "Guide for the Care and Use of Laboratory Animals" (Eighth Edition, 2011, Washington, D.C., National Academies Press, USA).

Consent for publication

Not applicable.

Availability of data and materials

The datasets used and/or analysed during the current study are available from the corresponding author on reasonable request.

Competing interests

The authors declare that they have no competing interests.

Funding

This study was supported by the National Natural Science Foundation of China (grant no. 81571886 and 81801905), Natural Science Foundation of Chongqing City (grant no. cstc2018jcyjAX0555), Major Program of Military Science Foundation of China during the 13th Five-Year Plan Period (grant no. AWS16J032), National Key Research and Development Program of China (grant no. 2017YFC1103302).

Authors' contributions

LY performed the experiments, analyzed the data, and drafted the manuscript. PXY and LT performed the experiments and analyzed the data. LLM contributed in experimental design and data analysis. YGM conceived and designed the research, analyzed the data, prepared figures, and finalized the manuscript. All authors read and approved final manuscript.

Acknowledgements

Not applicable.

References

1. Curry NS, Davenport R. Transfusion strategies for major haemorrhage in trauma. Br J Haematol. 2019;184(4):508-523.
2. Spahn DR, Bouillon B, Cerny V, Duranteau J, Filipescu D, Hunt BJ, Komadina R, Maegele M, Nardi G, Riddez L, Samama CM, Vincent JL, Rossaint R. The European guideline on management of major bleeding and coagulopathy following trauma: fifth edition. Crit Care. 2019;23(1):98.
3. Lei Y, Peng X, Li T, Liu L, Yang G. ERK and miRNA-1 target Cx43 expression and phosphorylation to modulate the vascular protective effect of angiotensin II. Life Sci. 2019;216:59-66.
4. Levy Bruno, Fritz Caroline, Tahon Elsa, Jacquot A, Auchet T, Kimmoun A . Vasoplegia treatments: the past, the present, and the future. Crit Care. 2018; 22(1):52.
5. Jentzer JC, Vallabhajosyula S, Khanna AK, Chawla LS, Busse LW, Kashani KB. Management of Refractory Vasodilatory Shock. Chest. 2018; 154(2):416-426
6. Yang G, Peng X, Hu Y, Lan D, Wu Y, Li T, Liu L. 4-Phenylbutyrate Benefits Traumatic Hemorrhagic Shock in Rats by Attenuating Oxidative Stress, Not by Attenuating Endoplasmic Reticulum Stress. Crit Care Med. 2016;44(7):e477-91.
7. Brown E M, Gamba G, Riccardi D, Lombardi M, Butters R, Kifor O, Sun A, Hediger MA, Lytton J, Hebert SC. Cloning and characterization of an extracellular Ca(2+)-sensing receptor from bovine parathyroid. Nature. 1993;366(6455):575-80.
8. Hannan FM, Kallay E, Chang W, Brandi ML, Thakker RV. The calcium-sensing receptor in physiology and in calcitropic and noncalcitropic diseases. Nat Rev Endocrinol. 2018;15(1):33-51.
9. Schreckenberg R, Schlüter KD. Calcium sensing receptor expression and signalling in cardiovascular physiology and disease. Vascul Pharmacol. 2018; doi:10.1016/j.vph.2018.02.007.
10. Jensen BL. Smelling through calcium-sensing receptor affects sympathetic control of blood pressure and regional blood flow. Acta Physiol (Oxf). 2019;225(1):e13180.
11. Schepelmann M, Yarova PL, Lopez-Fernandez I, Davies TS, Brennan SC, Edwards PJ, Aggarwal A, Graça J, Rietdorf K, Matchkov V, Fenton RA, Chang W, Krssak M, Stewart A, Broadley KJ, Ward DT, Price SA, Edwards DH, Kemp PJ, Riccardi D. The vascular Ca2+-sensing receptor regulates blood vessel tone and blood pressure. Am J Physiol Cell Physiol. 2016;310(3):C193-204.
12. Hannan FM, Olesen MK, Thakker RV. Calcimimetic and calcilytic therapies for inherited disorders of the calcium-sensing receptor signalling pathway. Br J Pharmacol. 2018;175(21):4083-4094.
13. Howles SA, Hannan FM, Babinsky VN, Rogers A, Gorvin CM, Rust N, Richardson T, McKenna MJ, Nesbit MA, Thakker RV. Cinacalcet for Symptomatic Hypercalcemia Caused by AP2S1 Mutations. N

Engl J Med. 2016;374(14):1396-1398.

14. Mohsin S, Baniyas MM, AlDarmaki RS, Tekes K, Kalász H, Adeghate EA. An update on therapies for the treatment of diabetes-induced osteoporosis. Expert Opin Biol Ther. 2019;19(9):937-948.
15. Sun R, Zhang W, Zhong H, Wang L, Tang N, Liu Y, Zhao Y, Zhang T, He F. Calcimimetic R568 reduced the blood pressure and improved aortic remodeling in spontaneously hypertensive rats by inhibiting local renin-angiotensin system activity. Exp Ther Med. 2018;16(5):4089-4099.
16. Greenberg HZE, Jahan KS, Shi J, Vanessa Ho WS, Albert AP. The calcilytics Calhex-231 and NPS 2143 and the calcimimetic Calindol reduce vascular reactivity via inhibition of voltage-gated Ca2+ channels. Eur J Pharmacol. 2016;791:659-668.
17. Bhatti JS, Bhatti GK, Reddy PH. Mitochondrial dysfunction and oxidative stress in metabolic disorders - A step towards mitochondria based therapeutic strategies. Biochim Biophys Acta Mol Basis Dis. 2017;1863(5):1066-1077.
18. Ježek J, Cooper KF, Strich R. Reactive Oxygen Species and Mitochondrial Dynamics: The Yin and Yang of Mitochondrial Dysfunction and Cancer Progression. Antioxidants (Basel). 2018;7(1) .
19. Cid-Castro C, Hernández-Espinosa DR, Morán J. ROS as Regulators of Mitochondrial Dynamics in Neurons. Cell Mol Neurobiol. 2018;38(5):995-1007.
20. Ren J, Yang L, Zhu L, Xu X, Ceylan AF, Guo W, Yang J, Zhang Y. Akt2 ablation prolongs life span and improves myocardial contractile function with adaptive cardiac remodeling: role of Sirt1-mediated autophagy regulation. Aging Cell. 2017;16(5):976-987.
21. Chavez-Abiega S, Mos I, Centeno PP, Elajnaf T, Schlattl W, Ward DT, Goedhart J, Kallay E. Sensing Extracellular Calcium - An Insight into the Structure and Function of the Calcium-Sensing Receptor (CaSR). Adv Exp Med Biol. 2020;1131:1031-1063.
22. Odenwald T, Nakagawa K, Hadtstein C, Roesch F, Gohlke P, Ritz E, Schaefer F, Schmitt CP. Acute blood pressure effects and chronic hypotensive action of calcimimetics in uremic rats. J Am Soc Nephrol. 2006;17(3) 655-662.
23. Ogata H, Ritz E, Odoni G, Amann K, Orth SR. Beneficial effects of calcimimetics on progression of renal failure and cardiovascular risk factors. J Am Soc Nephrol. 2003;14(4) 959-967.
24. Rybczynska A, Jurska-Jasko A, Boblewski K, Lehmann A, Orlewska C. Blockade of calcium channels and AT1 receptor prevents the hypertensive effect of calcilytic NPS 2143 in rats. J Physiol Pharmacol. 2010;61(2) 163-170.
25. Fryer RM, Segreti JA, Widomski DL, Franklin PH, Banfor PN, Koch KA, Nakane M, Wu-Wong JR, Cox BF, Reinhart GA. Systemic activation of the calcium sensing receptor produces acute effects on vascular tone and circulatory function in uremic and normal rats: focus on central versus peripheral control of vascular tone and blood pressure by cinacalcet. J Pharmacol Exp Ther. 2007;323(1) 217-226.
26. Zhao M, He X, Yang YH, Yu XJ, Bi XY, Yang Y, Xu M, Lu XZ, Sun Q, Zang WJ. Acetylcholine protects mesenteric arteries against hypoxia/reoxygenation injury via inhibiting calcium-sensing receptor. J Pharmacol Sci. 2015;127(4) 481-488.

27. Liesa M, Palacín M, Zorzano A. Mitochondrial dynamics in mammalian health and disease. Physiol Rev. 2009;89(3) 799-845.
28. Cao YL, Meng S, Chen Y, Feng JX, Gu DD, Yu B, Li YJ, Yang JY, Liao S, Chan DC, Gao S. MFN1 structures reveal nucleotide-triggered dimerization critical for mitochondrial fusion. Nature. 2017;542(7641) 372-376.

Figures

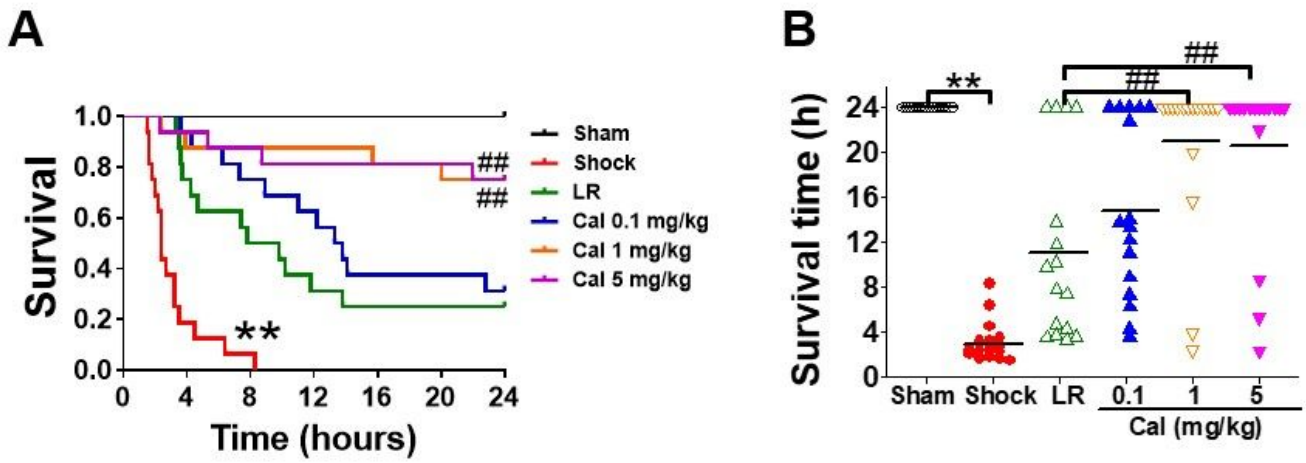

Figure 1

. Effect of Cal on survival after traumatic hemorrhagic shock. A: Kaplan-Meier survival curve. B: Survival time. Symbol colors are defined in the key in panel A. *P <0.05, **P <0.01 compared with the sham-operated group; # P <0.05, ## P <0.01 compared with the LR group. Sham, sham-operated; LR, lactated Ringer's solution; Cal, Calhex-231. n=16/group.

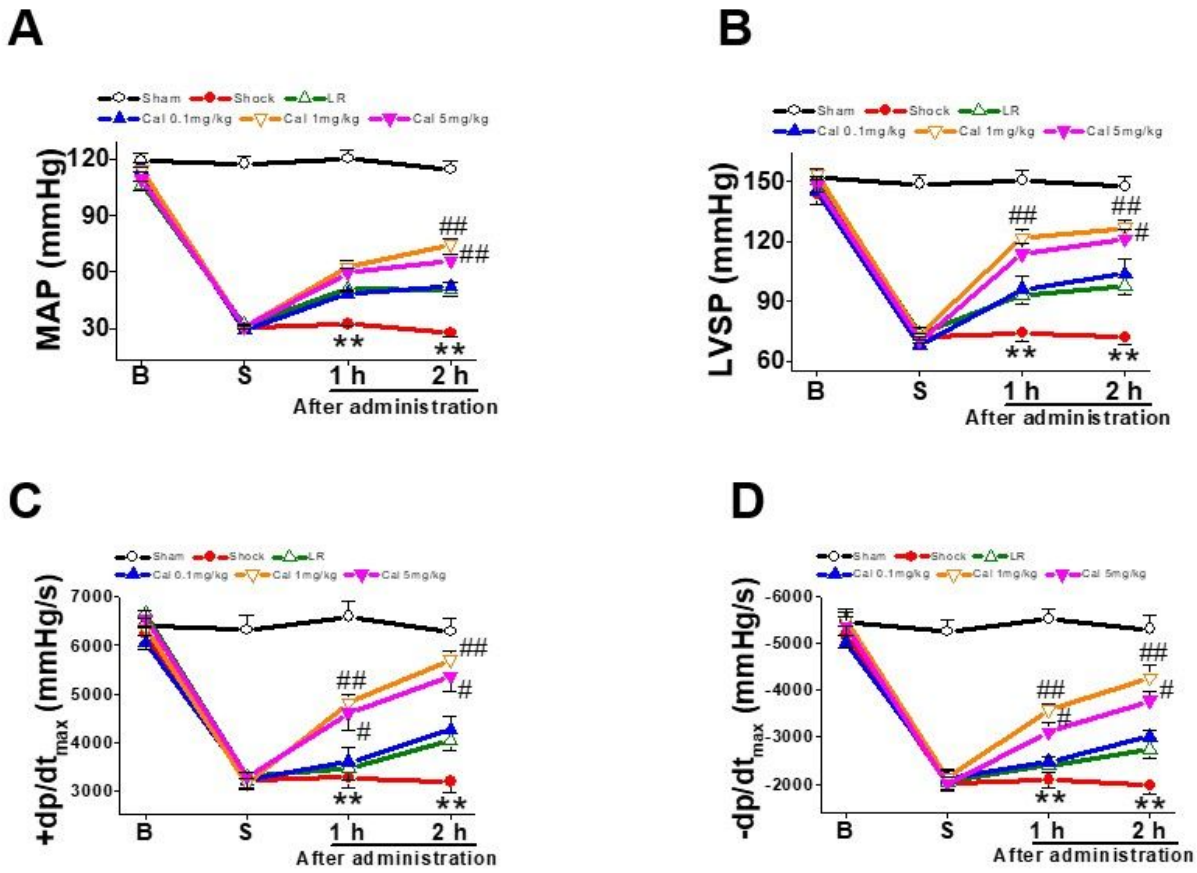

Figure 2

Effect of Cal on hemodynamic parameters after traumatic hemorrhagic shock. A: Mean arterial pressure (MAP). B: Left intraventricular systolic pressure (LVSP). C and D: Maximal change rate in left intraventricular pressure (±dp/dtmax). *P <0.05, **P <0.01 compared with the sham-operated group; # P <0.05, ## P <0.01 compared with the LR group. Sham, sham-operated; LR, lactated Ringer's solution; Cal, Calhex-231; B, baseline; S, shock. n=8/group.

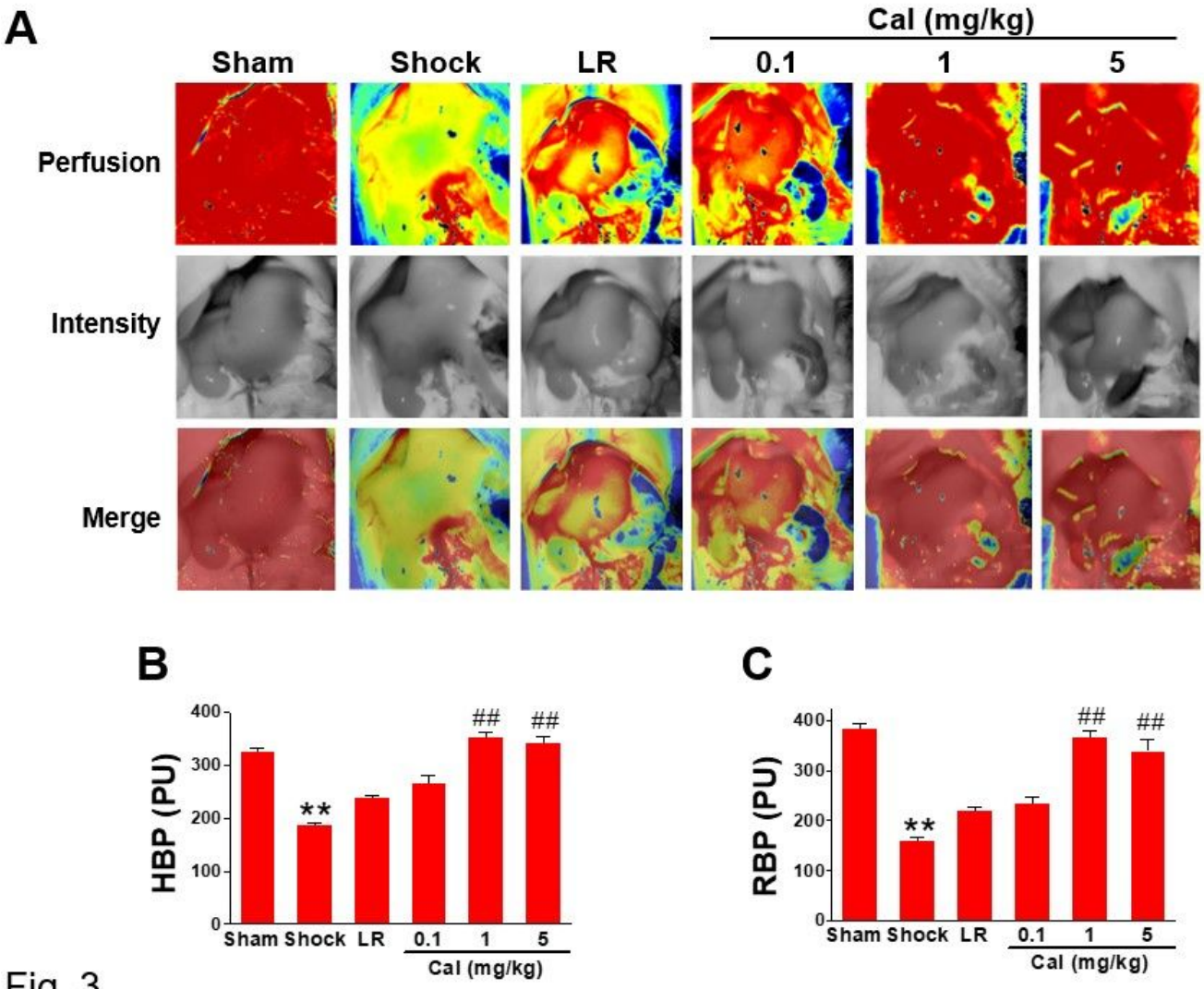

Fig. 3

Figure 3

Effects of Cal on blood perfusion and oxygen saturation of liver and kidney after THS. A: Representative LASCA images of blood perfusion in liver and kidney. B and C: Graphical representation and statistical analysis of hepatic (HBP) and renal blood perfusion (RBP). D and E: Oxygen saturation of liver and kidney. *P <0.05, **P <0.01 compared with the sham-operated group; # P <0.05, ## P <0.01 compared with the LR group. Sham, sham-operated; LR, lactated Ringer's solution; Cal, Calhex-231. n=8/group.

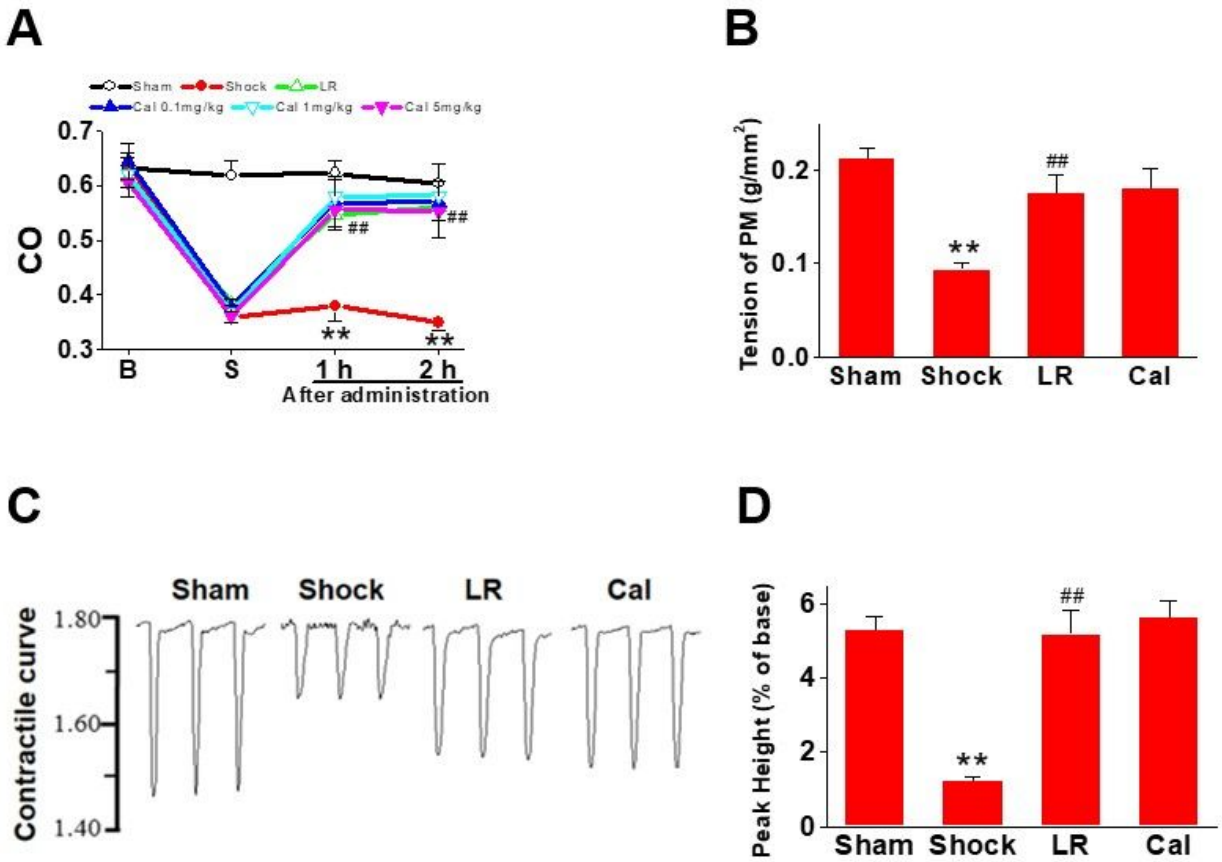

Fig. 4

Figure 4

Effect of Cal on cardiac function after traumatic hemorrhagic shock. A: Cardiac output (CO). B: Contractility of isolated ventricular papillary muscle (PM). C: Representative curves of cardiomyocyte contraction. D: Contractility of single cardiomyocytes. *P <0.05, **P <0.01 compared with the sham-operated group; # P <0.05, ## P <0.01 compared with the LR group. Sham, sham-operated; LR, lactated Ringer's solution; Cal, Calhex-231; B, baseline; S, shock. n=8/group.

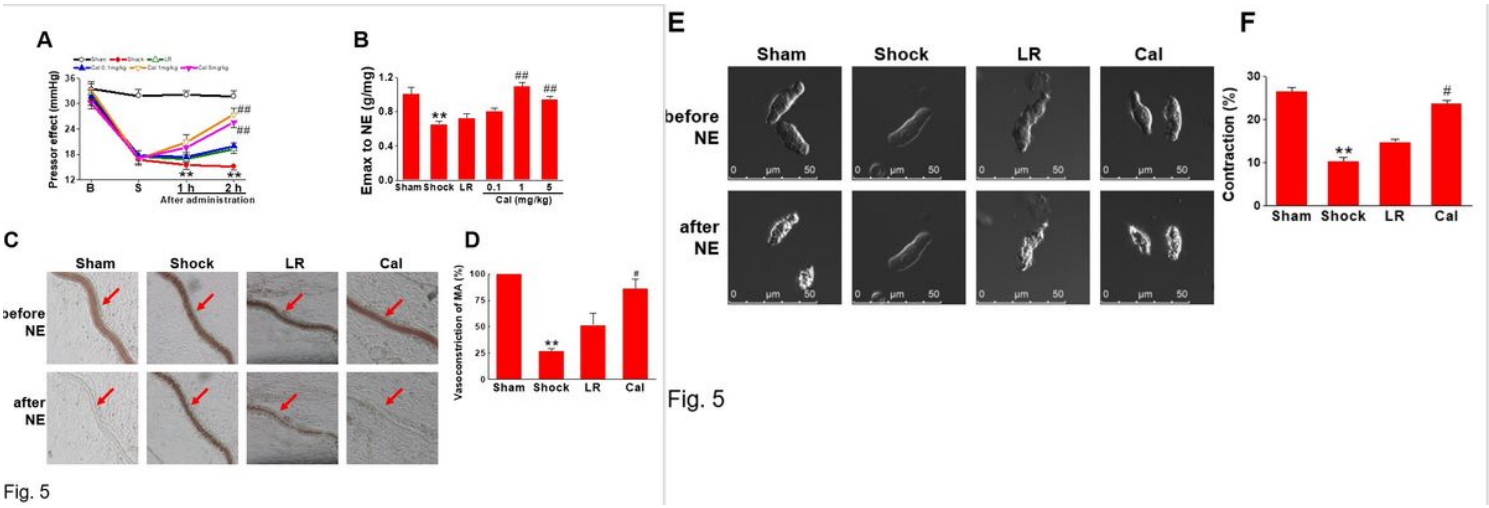

Figure 5

Effects of Cal on vascular function after traumatic hemorrhagic shock. A: Pressor effect of norepinephrine (NE). B: Contractile response of superior mesenteric arteries (SMA) to NE. C and D: Contractile response of mesenteric arterioles (MA) to NE. E and F: Contractility of single VSMCs. *P <0.05, **P <0.01 compared with the sham-operated group; # P <0.05, ## P <0.01 compared with the LR group. Sham, sham-operated; LR, lactated Ringer's solution; Cal, Calhex-231; B, baseline; S, shock. n=8/group.

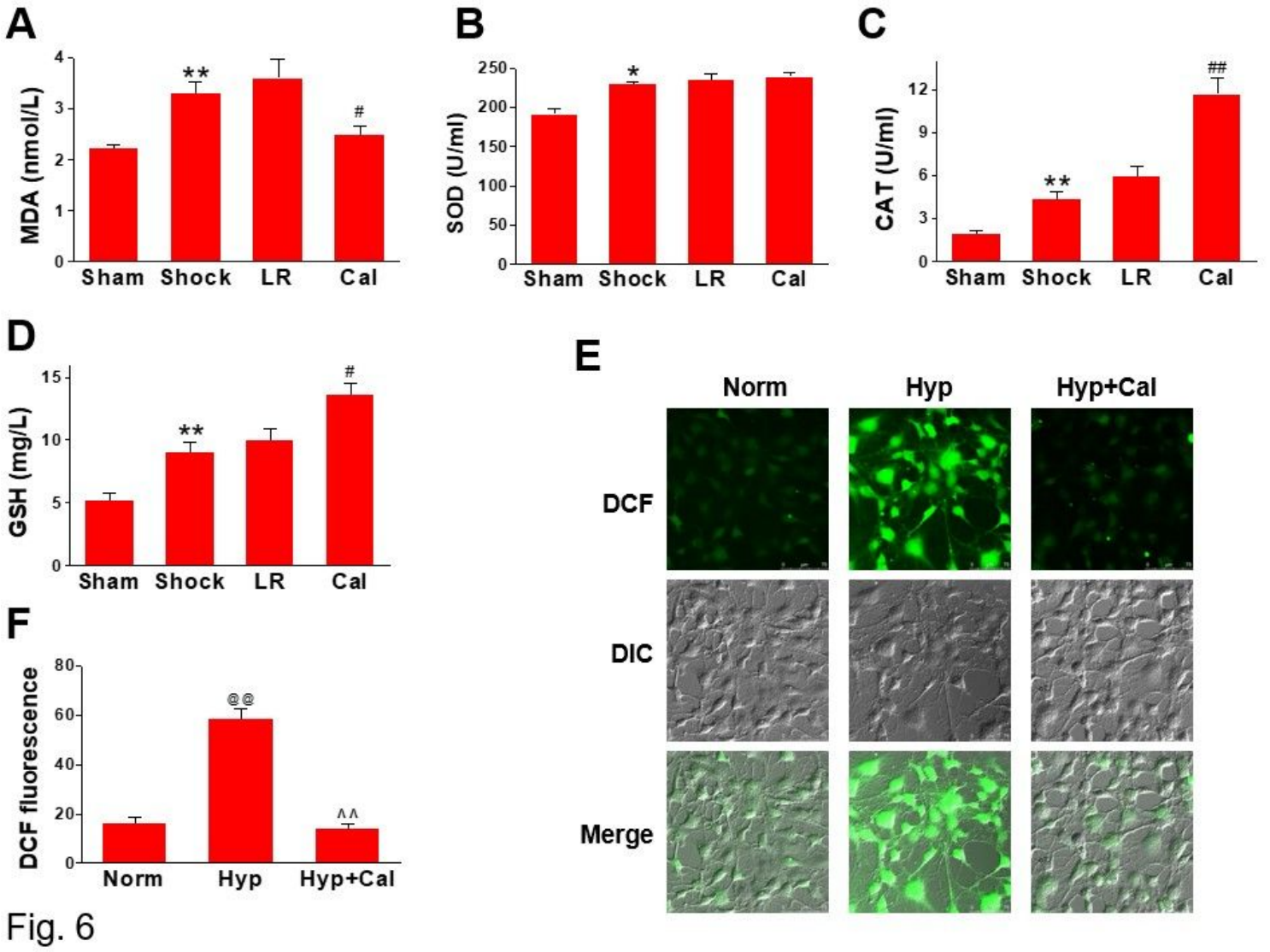

Fig. 6

Figure 6

Effects of Cal on oxidative stress in vivo and in vitro. A-D: Levels of malondialdehyde (MDA), superoxide dismutase (SOD), catalase (CAT), and glutathione (GSH) in blood samples (n=8/group). E: Images acquired by confocal microscopy showing intracellular ROS levels in VSMCs. F: Quantitative data of the mean intensity of 2',7'-dichlorofluorescin (DCF, a probe of ROS) fluorescence (n=30 cells/group). *P <0.05, **P <0.01 compared with the sham-operated group; # P <0.05, ## P <0.01 compared with the LR group; @ P <0.05, @@ P <0.01 compared with the normal group; ^ P <0.05, ^^ P <0.01 compared with the hypoxia group. Sham, sham-operated; LR, lactated Ringer's solution; Cal, Calhex-231; Norm, normal; Hyp, hypoxia.

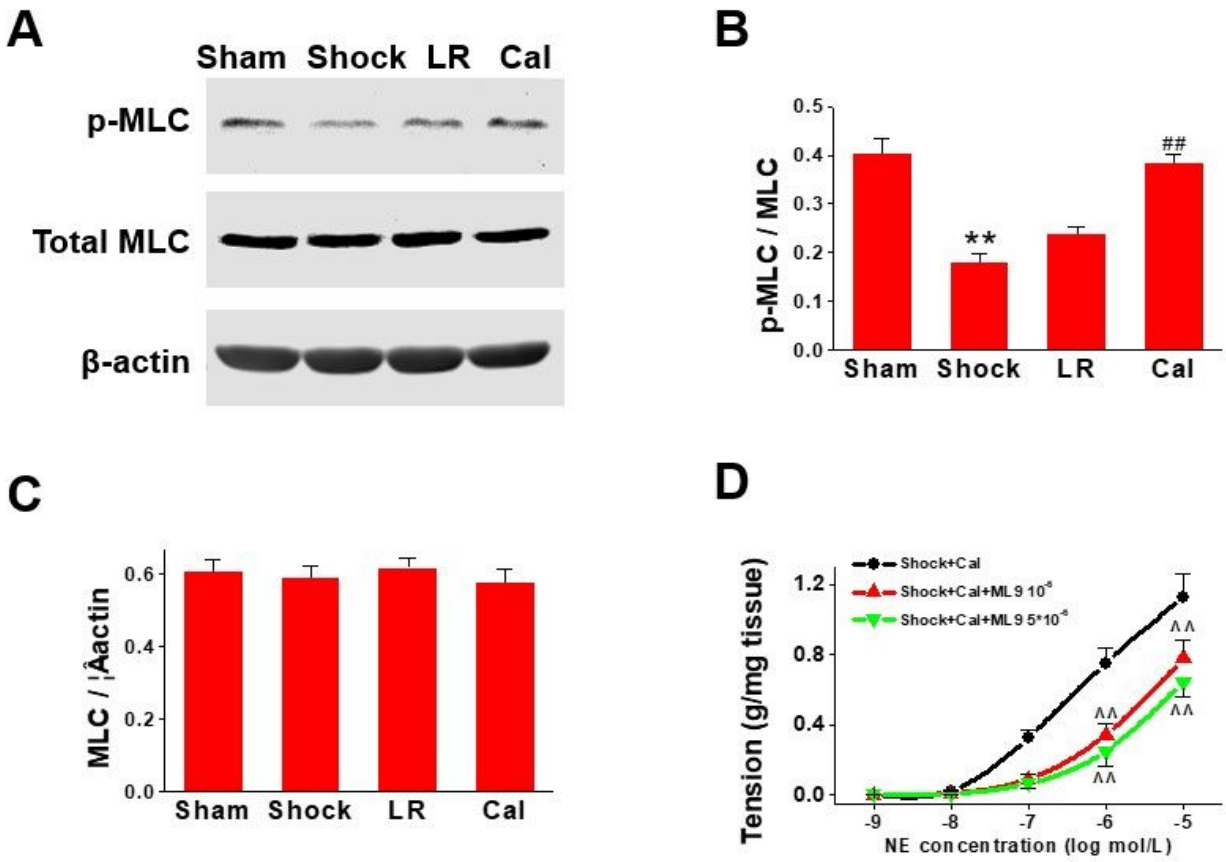

Figure 7

Relationship between MLC phosphorylation and effects of Cal on vascular reactivity after THS. A: Representative immunoblots showing the expression and phosphorylation of MLC. B: Ratio of phosphorylated MLC/total MLC based on optical density of immunoblot bands. C: Ratio of total MLC/β-actin based on optical density of immunoblot bands. Immunoblot analyses were repeated three times. D: Contractile response of superior mesenteric arteries to norepinephrine (NE) (n=8/group). *P <0.05, **P <0.01 compared with the sham-operated group; # P <0.05, ## P <0.01 compared with the LR group; ^ P <0.05, ^^ P <0.01 compared with the shock+Cal group. Sham, sham-operated; LR, lactated Ringer's solution; Cal, Calhex-231.

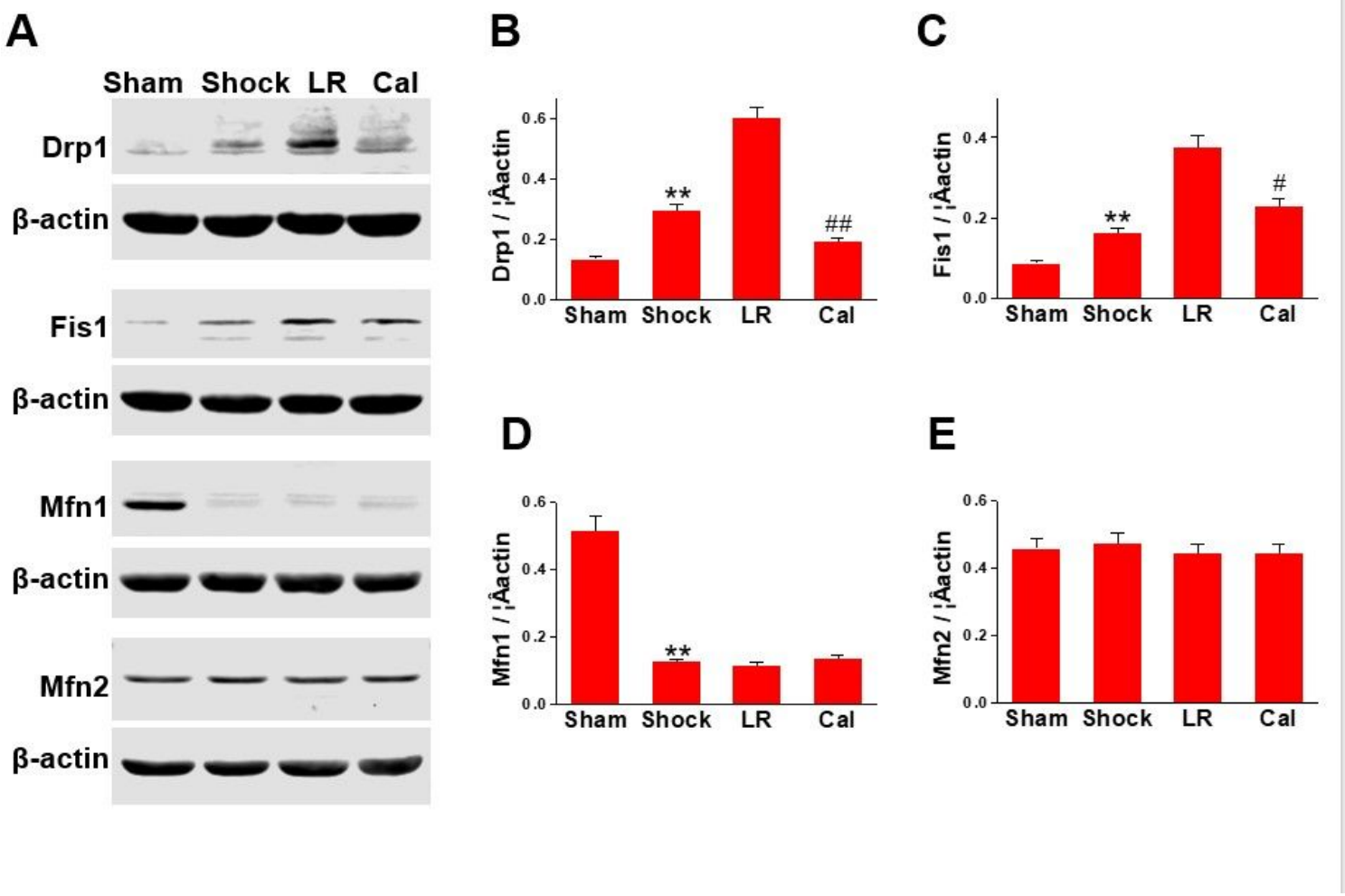

Figure 8

Effects of Cal on mitochondrial fission/fusion and mitochondrial morphology following THS. A: Representative immunoblots showing expression of Drp1, Fis1, Mfn1, and Mfn2. B-E: Protein levels normalized to β-actin based on optical density of immunoblot bands. Immunoblot analyses were repeated three times. F: Representative confocal images showing morphology of rat VSMC mitochondria stained with MitoTracker deep red. Red: MitoTracker fluorescence; blue: DAPI fluorescence. The boxed areas in the top images are shown at higher magnification in the bottom images. Experiments were repeated three times. *P <0.05, **P <0.01 compared with the sham-operated group; # P <0.05, ## P <0.01 compared with the LR group. Sham, sham-operated; LR, lactated Ringer's solution; Cal, Calhex-231; Norm, normal; Hyp, hypoxia.